A Whole-Cell and Single-Channel Study of the Voltage-dependent Outward Potassium Current in Avian Hepatocytes

CARLA MARCHETTI, RICHARD T. PREMONT, and ARTHUR M. BROWN

From the Department of Physiology and Molecular Biophysics and the Department of Cell Biology, Baylor College of Medicine, Houston, Texas 77030

ABSTRACT Voltage-dependent membrane currents were studied in dissociated hepatocytes from chick, using the patch-clamp technique. All cells had voltage-dependent outward K^+ currents; in 10% of the cells, a fast, transient, tetrodotoxin-sensitive Na^+ current was identified. None of the cells had voltage-dependent inward Ca^{2+} currents. The K^+ current activated at a membrane potential of about −10 mV, had a sigmoidal time course, and did not inactivate in 500 ms. The maximum outward conductance was 6.6 ± 2.4 nS in 18 cells. The reversal potential, estimated from tail current measurements, shifted by 50 mV per 10-fold increase in the external K^+ concentration. The current traces were fitted by n^2 kinetics with voltage-dependent time constants. Omitting Ca^{2+} from the external bath or buffering the internal Ca^{2+} with EGTA did not alter the outward current, which shows that Ca^{2+}-activated K^+ currents were not present. 1–5 mM 4-aminopyridine, 0.5–2 mM $BaCl_2$, and 0.1–1 mM $CdCl_2$ reversibly inhibited the current. The block caused by Ba was voltage dependent. Single-channel currents were recorded in cell-attached and outside-out patches. The mean unitary conductance was 7 pS, and the channels displayed bursting kinetics. Thus, avian hepatocytes have a single type of K^+ channel belonging to the delayed rectifier class of K^+ channels.

INTRODUCTION

Membrane potential is important in regulating metabolic processes in the liver, including gluconeogenesis (Friedmann et al., 1971; Friedmann and Dambach, 1980), amino acid transport (Wondergem and Harper, 1980), and the rate of uptake of bile salts (Edmondson et al., 1985). Changes in K^+ permeability can affect the transmembrane potential, independently of Na^+,K^+-ATPase activity (Haber and Loeb, 1986). A number of agents, including α-adrenoreceptor agonists (Burgess et al., 1981; DeWitt and Putney, 1984), insulin, and glucagon (Williams et al., 1971; Somlyo et al., 1971), have been shown to act on liver cell

Address reprint requests to Dr. Arthur M. Brown, Dept. of Physiology and Molecular Biophysics, Baylor College of Medicine, 1 Baylor Plaza, Houston, TX 77030. Dr. Marchetti's permanent address is Istituto di Cibernetica e Biofisica, Consiglio Nazionale delle Richerche, Genoa, Italy.

J. GEN. PHYSIOL. © The Rockefeller University Press · 0022-1295/88/02/0255/20 $2.00

Volume 91 February 1988 255–274

membranes by altering K^+ fluxes. The introduction of the patch-clamp method has made the electrophysiology of many tissues more accessible to experimental study. One result is an awakened interest in the function of voltage-dependent ionic channels in nonexcitable cells. In particular, voltage-dependent K^+ channels have been described in lymphocytes (Cahalan et al., 1985), macrophages (Ypey and Clapham, 1984), natural killer cells (Schlichter et al., 1986), and a variety of epithelial cells (reviewed in Van Driessche and Zeiske, 1985). The K^+-selective channels described in these preparations vary greatly in their voltage dependence, conductance, and Ca^{2+} requirements. Evidence has accumulated for a Ca^{2+}-sensitive K^+ conductance in the guinea pig liver that would mediate the action of Ca^{2+}-mobilizing chemical transmitters such as α-adrenergic agonists and vasopressin (Burgess et al., 1981; DeWitt and Putney, 1984; Cook and Haylett, 1985). This mechanism is, however, absent in the rat liver (Burgess et al., 1981; Berthon et al., 1985). Although inferences can be drawn from these reports, the ionic channels of liver cell membranes have never been investigated directly.

Parenchymal cells (hepatocytes) dispersed with collagenase from chick livers survive well in culture for 4–5 d and retain the morphological and lipogenic properties of the in vivo liver (Tarlow et al., 1977). We took advantage of this to investigate the ionic channels present in these cells. We have identified a K^+-permeable, voltage-dependent, 4-aminopyridine–sensitive channel of the delayed rectifier type. The outward K^+ current was independent of the external Ca^{2+} concentration, which correlates with the fact that no voltage-dependent Ca^{2+}-selective channels were identified. The K^+ conductance is active near the resting membrane potential and might be implicated in the control of resting potential.

MATERIALS AND METHODS

Cell Isolation and Culture

Hepatocytes were prepared by collagenase digestion, using a procedure similar to those described by Tarlow et al. (1977) and by Watkins et al. (1977). Collagenase (type CLS III, Cooper Biomedical, Inc., Malvern, PA) was dissolved in phosphate-buffered saline (PBS) to a concentration of 50 U/ml, with 10 μg/ml soybean trypsin inhibitor (Sigma Chemical Co., St. Louis, MO) and 50 mM glucose; DNaseI (Sigma Chemical Co.) was dissolved in 1 mM HCl (2.5 mg/ml). Erythrocyte lysis buffer contained 140 mM NH_4Cl and 17 mM Tris HCl. The pH was 7.2. Basal Eagle's medium (BME) and phosphate-buffered Eagle's medium (EPB) were as given by Watkins et al. (1977).

Livers were dissected from 12–14-d-old female white leghorn chicks, rinsed in sterile PBS at room temperature, and finely minced with scissors. The mince was incubated in 30 ml collagenase and 1 ml DNase solution for 20 min at 37°C on a rotary shaker (250 cycles/min). The supernatant was spun for 3 min at 1,000 *g*, and the cell pellets were resuspended in 20 ml EPB. The 20-min incubation was repeated with the remaining liver mince. At the end of the second incubation, the collagenase-digested tissue was filtered through a 100-mesh silk screen (0.006 in.) to remove undigested tissue, and the filtrate was spun down as before and resuspended in 20 ml EPB. The first and second cell suspensions were pooled, spun down, and resuspended in 20 ml erythrocyte lysis buffer for 5 min. The cells were washed twice in 20 ml EPB and filtered again through a silk screen. The cells in the final suspension were counted with a hemocytometer and immediately adjusted to 2×10^6 cells/ml in warm BME supplemented with 5% chicken serum and 5 μg/ml insulin. The viability, tested by trypan blue exclusion, was 85–90%.

For electrophysiological experiments, the cells were diluted to a density of 5×10^5/ml in the same BME medium with serum and insulin and plated on polylysine-coated glass coverslips in 35-mm Falcon culture dishes. Cells were stored in a water-jacketed incubator in 10% CO_2 atmosphere at 37°C for at least 24 h before use. Media were changed 18 h after the initial plating and every 24 h thereafter.

Previous studies using primary cultures of chick hepatocytes have noted the retention of several characteristics of differentiated hepatocyte function, including hormonally regulated lipogenesis (Tarlow et al., 1977; Watkins et al., 1977) and ligand-dependent down-regulation of insulin receptors (Krupp and Lane, 1981). Further studies on the regulation of the glucagon receptor, in the same preparations used for the electrophysiological studies, have demonstrated a retention of in vivo levels and activities of the component of the glucagon-stimulated adenyl cyclase system for the 5-d culture period (Premont, R., and R. Iyengard, unpublished results).

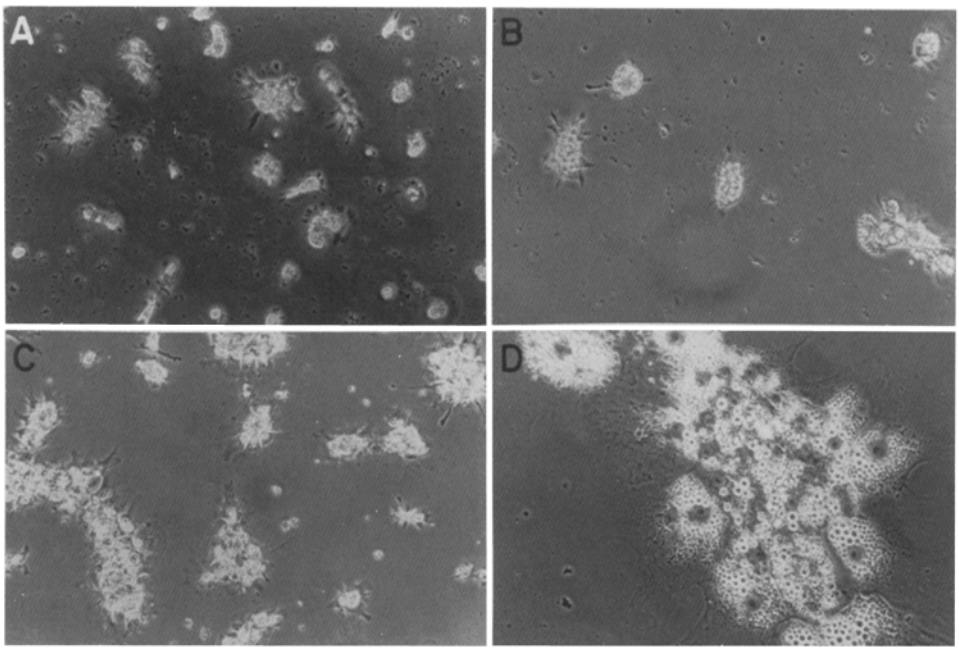

Photographs of the cell monolayer 48 and 84 h after dissociation are shown in Fig. 1. Cells began to form clusters between 24 and 48 h after plating, and the cells in those clusters were electrically coupled, as judged by the long time constant of the passive electrical response. Isolated cells had to be used for electrical recording because electrical coupling did not allow satisfactory voltage control. At the low density used for our studies, the monolayer did not reach confluency, and isolated cells suitable for recording could be found even after 4 d in culture. However, the best time for recording was between 36 and 72 h after dissociation. After this time, most of the cells were flat and coupled, and the remaining round, uncoupled cells were found to have resting potentials near 0 mV.

Electrophysiology

Membrane ionic currents were measured in the standard whole-cell patch-clamp configuration as described by Hamill et al. (1981). Patch electrodes, pulled from glass capillaries

(TW150, World Precision Instruments, Inc., Hamden, CT), had resistances of 2–4 MΩ when filled with the standard 140 mM KCl internal solution (see Table I) and 3–6 MΩ when aspartate was the main anion. The voltage-clamp amplifier was an EPC-7 (List-Medical Systems, Darmstadt, Federal Republic of Germany). Capacitance artifacts were compensated by an analog circuit, and the value of the compensated capacitance was taken as an estimate of the cell capacitance. The series resistance increased at least three times when the whole-cell recording was established, but it was compensated up to 80%. Data were filtered by a four-pole Bessel filter with a cutoff of 5 kHz, and digitized on-line by a computer (LSI 11/73, Digital Equipment Corp., Marlboro, MA) at a frequency of 50–100 μs/point. Because compensation of the series resistance introduces additional noise in the range 2–5 kHz, the current records were subsequently filtered at 2 kHz, using a zero-phase digital filter (Brown et al., 1984; Lux and Brown, 1984). The frequency of stimulation was one pulse every 5 s, unless otherwise stated. Leak current was estimated by extrapolating a line through current recorded at subthreshold potentials and was assumed to be linear through the entire voltage range. The maximum conductance was

TABLE I

*Solutions**

External solutions	NaCl	KCl	$CaCl_2$	$MgCl_2$	Glucose	HEPES	EGTA
Standard external (Tyrode)	135	5.4	1.8	2	10	5	—
Ca^{2+}-free Tyrode	135	5.4	—	2	10	5	1
Ca^{2+}-free high-Mg^{2+}	130	5.4	—	8	10	5	1

Internal solutions	KCl	$MgCl_2$	EGTA	HEPES	CsCl	CsAsp
Standard internal	140	1	—	5	—	—
Internal 2 EGTA	140	1	2	5	—	—
Cs internal	—	1	5	5	20	110

* All values are in millimolar units.

calculated from the corrected current amplitude at the most depolarized potential, assuming an average reversal potential of −70 mV, in the standard conditions (see discussion in Results). Leak current and the residual capacitive artifact were digitally subtracted from each record, using the response to either subthreshold or hyperpolarizing voltage pulses, appropriately scaled. Corrected traces were fitted to models, and the fits were optimized using the nonlinear least-squares of Marquandt, as described in Bevington (1969).

Single-channel recording was performed in the cell-attached and outside-out configurations under the same conditions as the whole-cell clamp, except that the gain was 200 pA–1 nA/V for whole-cell currents and 10 pA/V for single-channel currents. Data were digitized at a frequency of 100 μs/point. The capacitive current artifact was corrected using the means of current traces that did not contain any activity. Idealized traces were calculated from the corrected traces using an interactive routine. Histograms of amplitude, open time, and closed time were constructed from the idealized traces and fitted with Gaussian curves or single or double exponentials, respectively.

Solutions and Drugs

The solutions used are listed in Table I. The pH was adjusted to 7.4 with Tris base, and the osmolarity was 290 ± 10. The majority of the experiments were performed in a

standard (Tyrode) external bath and with a 140 mM KCl solution, containing neither EGTA nor Ca^{2+} in the pipette. To study the reversal potential shift with increasing concentrations of K^+ in the external medium, the Na^+ concentration was reduced appropriately to preserve osmolarity.

All of the drugs used in this study, 4-aminopyridine (4-AP), apamin, and tetrodotoxin (TTX), as well as the hormones insulin, glucagon, and phenylephrine, were purchased from Sigma Chemical Co. They were made up at the desired concentration in the control bath solution, applied by continuous perfusion, and washed out in the same way.

RESULTS

Passive Properties

High-resistance (≥10 GΩ) seals were formed on nearly all of the cells with application of gentle suction to the interior of the pipette. In a significant number of cases (10–15%), gigaseals formed spontaneously upon apposition of the glass tip to the membrane. When suction was increased, the membrane ruptured, with an immediate increase of the capacitance transient amplitude and time constant. Typical values of the input resistance immediately after the cell was broken into were 0.2–1.5 GΩ, corresponding to a resting input conductance of 0.6–5 nS. The leak current was linear in the range −100 to −20 mV and, when isolated by blocking the voltage-dependent current with internal Cs^+ (see below), proved to be linear up to 30 mV. We considered this current to be "nonspecific" and it was not investigated further.

The membrane capacitance was 14.4 ± 3.6 pF in 24 cells. Because of the irregular shape of the cells (see Fig. 1), it was impossible to estimate the geometric area of the cell that contributed to the capacitance.

The resting potential of the hepatocytes was measured in the current-clamp mode, with zero current applied, or in the voltage-clamp mode, taking it as the potential at which the leak current was zero. The resting potential ranged between −25 and −15 mV, values that are in good agreement with those found by other authors (Wondergem and Harper, 1980; Wondergem, 1983) in isolated hepatocytes. An important exception was found in cultures grown in the presence of glucagon (5 nM). Under these conditions, a membrane potential of −50 ± 5 mV was measured in seven cells. The observation that glucagon caused a stable hyperpolarization of liver cells has been reported previously by other authors (Petersen, 1974; Friedmann and Dambach, 1980; Edmondson et al., 1985).

Membrane Currents

Fig. 2*A* shows a set of current records obtained from a cell held at −50 mV. Depolarizing voltage increments evoked a voltage-dependent outward current that activated with a sigmoidal time course at a membrane potential of −10 mV. This current was found in all of the cells tested ($n = 85$), regardless of their age in culture. The leak current was digitally subtracted from these records, using the responses to hyperpolarizing voltage pulses. The effect of the subtraction is illustrated in Fig. 2*B*, where two *I-V* curves, before and after the correction, are shown. In the uncorrected plot (*A*, right-hand panel), a line can be extrapolated through the current values more negative than −20 mV.

The reversal potential of the outward current was estimated by measuring tail currents. Fig. 3*A* shows the tail current for repolarization in the range of −20 to −80 mV. The quasi-instantaneous *I-V* relation was linear in this range. The reversal potential was −80 mV, which is close to the theoretical Nernst potential for a K^+-selective channel.

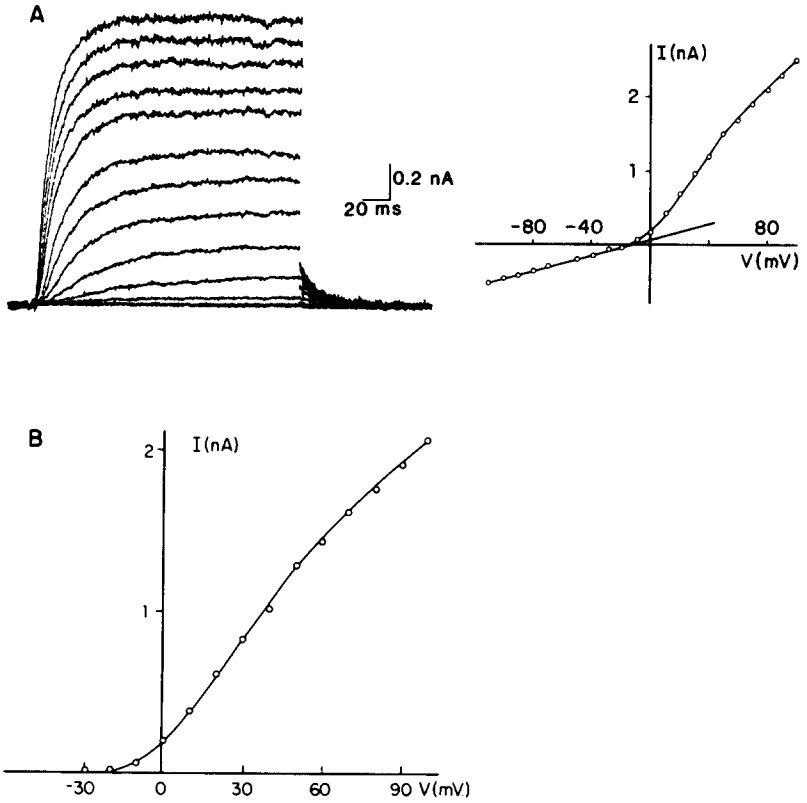

FIGURE 2. (*A*) Outward currents from an isolated hepatocyte bathed in standard external (Tyrode) solution. The internal (pipette) solution contained 140 mM KCl, with no EGTA added (see Table I). Depolarizing voltage pulses were applied every 5 s for 200 ms from a holding potential of −50 mV, in 10-mV increments. The maximum current shown corresponds to a voltage pulse to 90 mV. The leak current has been digitally subtracted from each record. (*Inset*) The *I-V* relation before leak subtraction shows how a line can be extrapolated through the current values at subthreshold potentials. (*B*) *I-V* relation from the same cell.

Fig. 3*B* shows the effect of substituting a 140 mM KCl solution, which is identical to that used to fill the pipette, in the external bath. The reversal potential was 0 ± 5 mV in these conditions (four cells). External solutions that contained different concentrations of K^+ were used to determine the relation between $\ln[K^+]_o$ and E_K. Fig. 3*D* shows the results obtained in four different cells. The points are fitted well by a straight line, and the reversal potential

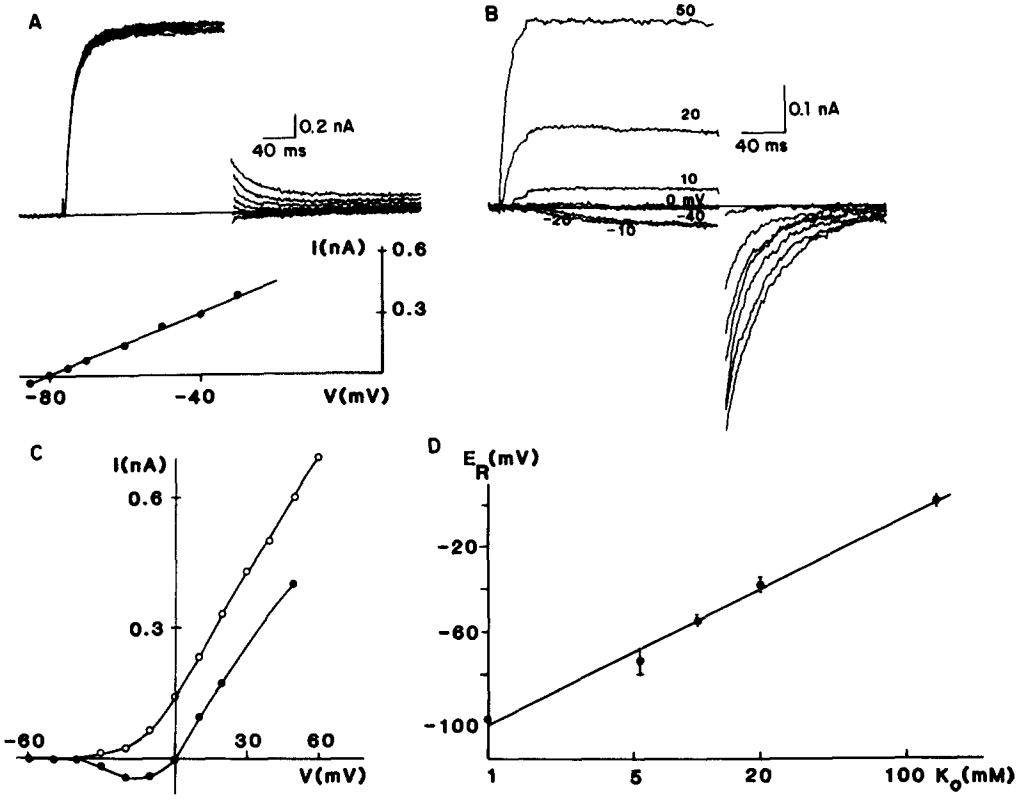

FIGURE 3. (*A*) Top: tail currents at different repolarization potentials. The cell was maintained at −50 mV, and a depolarizing pulse to +90 mV was applied for 200 ms, followed by a second pulse that varied in amplitude. The traces shown are relative to repolarization to −80, −75, −70, −60, −50, −40, and −30 mV. Internal and external solutions as in Fig. 1. Bottom: quasi-instantaneous *I-V* relation for the outward current, constructed from the tail currents in *A*. The relationship is linear, with a slope of 7.5 nS. The reversal potential is −80 mV. (*B*) Currents from an isolated hepatocyte in symmetrical 140 mM KCl solutions. The holding potential was −80 mV. (*C*) *I-V* relation for the current in standard conditions (open circles) and in symmetrical KCl (filled circles). In the latter condition, the current reversed at 0 mV. (*D*) Semilogarithmic plot of the reversal potential vs. the external K^+ concentration. Points represent averages and bars represent standard deviations in four cells. The linear regression through the experimental points gives a change of 50 mV in reversal potential for a 10-fold increase in the external K^+ concentration.

shifted by 50 mV per 10-fold increase in the external K^+ concentration. This observation justifies the assumption that the outward current was carried mainly by K^+.

From the linear fit of Fig. 3*D*, it was assumed that the reversal potential of the outward current was −70 mV in standard conditions (140 mM K^+ internal, 135 mM Na^+, 5.4 mM K^+ external), and this value was used to calculate the maximum

conductance. After the leak current was subtracted, the maximum conductance in 18 cells at command potentials greater than or equal to +50 mV was 6.6 ± 2.4 nS. When normalized to the membrane capacitance, this value gives a conductance of 436 ± 101 pS/pF or 436 ± 101 $\mu S/cm^2$, assuming a specific capacitance of 1 $\mu F/cm^2$.

Kinetics

The outward current was fully activated at 200 ms, and inactivation was negligible in 500 ms (not shown). We chose to fit the time course of activation of the current with Hodgkin-Huxley–type kinetics and found that an exponent $n = 2$ gave an adequate fit. Fig. 4 shows the best fit of currents from membrane potentials of −10 to +50 mV with the equation:

$$I = I_o \cdot [1 - \exp(-t/\tau_n)]^2.$$

The voltage dependence of τ_n in different cells is shown in Fig. 5. Tail currents were fitted best by a single-exponential decay. In four cells, the time constant for repolarization to −50 mV was $\tau = 22.03 \pm 3.12$ ms.

Ca^{2+} Dependence of the Outward Current

The influence of Ca^{2+} on the outward current was investigated with three different experiments. When the external bath was changed from a 2 mM Ca^{2+} solution to a Ca^{2+}-free solution containing 1 mM EGTA, the outward current recorded during the first few minutes of perfusion did not differ significantly from control, but the perfusion caused a sudden and irreversible increase of leak (not shown). The same experiment was performed using an external Ca^{2+}-free bath that contained 8 mM $MgCl_2$. The leak current was not affected in this case. Fig. 6*A* shows that this substitution caused a hyperpolarizing shift of ~10 mV in the activation of the outward current. If the correction for this shift is applied, the two *I-V* curves almost overlap (broken line). Fig. 6*B* shows the effect of internal EGTA (2 mM). In these conditions, the free Ca^{2+} concentration is $<10^{-9}$ M, assuming a dissociation constant of the Ca^{2+}-EGTA complex of 10^{-7} M and a concentration of Ca^{2+} in the absence of EGTA of 10^{-5} M. *I-V* relations from two different cells are compared, with and without EGTA in the pipette solution. Since there were no major differences between these two conditions, there were no indications that the outward current depended on intracellular Ca^{2+}.

Dependence on the Holding Potential

If the current was measured immediately after the cell was broken into, the outward current seemed to be independent of the holding potential and the currents recorded from a holding potential of −20 mV were indistinguishable from those from −50 mV. However, when the −20-mV holding potential was maintained, a slow inactivation of the outward current always occurred in the first 5–10 min, independently of the pulse frequency. Fig. 7*A* shows the decrease of the outward current as a function of time, for a cell held at −20 mV. The current recovered completely when the holding potential was set to a more

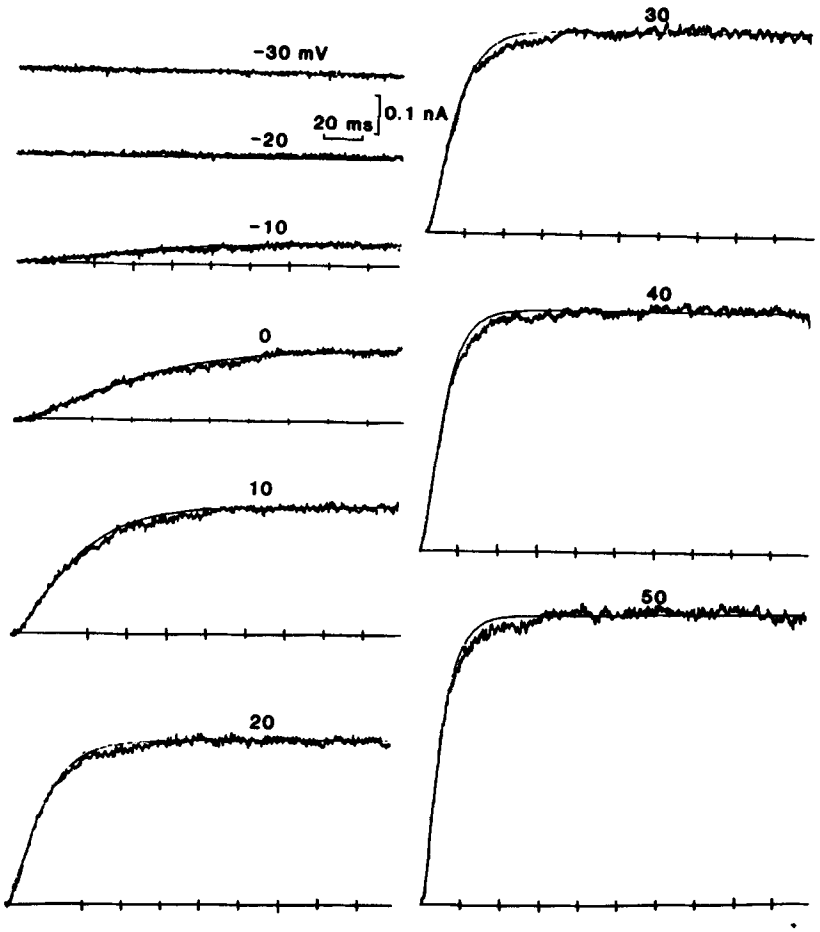

FIGURE 4. Fits of the outward current records with n^2 kinetics. Currents were recorded using the same solution conditions as in Fig. 2; the holding potential was −50 mV. The solid line is the fit. See text for explanation.

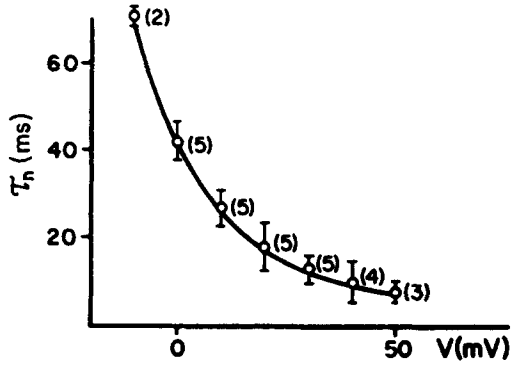

FIGURE 5. Voltage dependence of the time constant of activation, τ_n. The numbers in parentheses represent the numbers of values from different cells averaged. The points are connected for clarity.

negative value, −50 mV (indicated by the arrow). Another, faster, voltage-dependent inactivation was also observed several minutes after the cell was broken into. Fig. 7*B* shows the amplitude of outward current recorded at 40 mV following a 500-ms prepulse to different holding potentials. The current was not completely inactivated at −20 mV and the difference between the current from each more negative holding potential and the residual current from −20 mV was fitted with a sigmoidal curve, with the midpoint at −44 mV. When the holding potential was set to −50 mV, the outward current persisted for up to 80

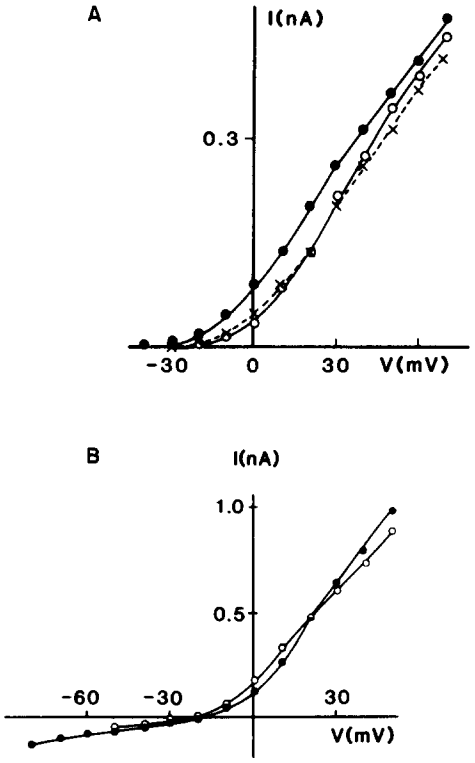

FIGURE 6. Effects of external and internal Ca^{2+} concentrations on the outward current. In *A*, the external bath was changed from a standard Tyrode (open circles) to a Ca^{2+}-free solution that contained 8 mM $MgCl_2$ (filled circles), and the *I-V* relation in these two conditions is shown. The pipette solution was standard internal, with no EGTA. The leak current was stable and was digitally subtracted from the records before the plot was calculated. If a 10-mV shift in activation is taken into account, the two curves overlap (broken line and ×'s). In *B*, the *I-V* relations from two different cells are shown. The open circles are from a cell perfused internally with a 140 mM KCl solution that did not contain EGTA; the filled circles are from a different cell, and the internal solution contained 2 mM EGTA (no Ca^{2+} added). The two cells were chosen because the amplitudes of their outward currents were comparable (data not normalized). The bath solution was standard Tyrode. The leak current was not subtracted.

min, but its amplitude was always smaller than that of the current from a holding potential of −80 mV. Because prolonged hyperpolarization could not be maintained easily, the holding potential was maintained at −50 mV in most of the experiments.

Effect of Blockers

Fig. 8, *A* and *B*, shows that the K^+ current was inhibited by 4-AP, an agent that is known to block voltage-dependent delayed rectifier K^+ channels (Yeh et al., 1976). The inhibition was reversible in the example shown, but irreversible in three other cells tested with higher doses (2–5 mM). This frequent lack of

reversibility may be related to the location of the 4-AP–binding site inside the channel, as postulated for the squid axon K^+ channel.

Fig. 9, *A* and *B*, shows the inhibition of the outward current caused by external $BaCl_2$ (2 mM). From a holding potential of −80 mV, the inhibition was voltage dependent and decreased exponentially with increasing depolarization (Fig. 9*C*). The outward current at 10 mV was reduced to 7% of the control value. From a holding potential of −50 mV, the current at 10 mV was reduced to 22% of control, and the voltage dependence of the block was negligible. These results agree with observations of other authors who used different preparations (Arm-

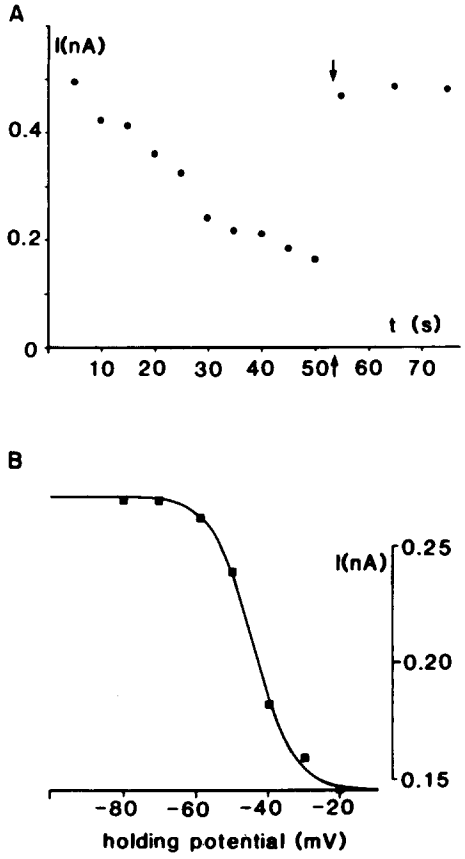

FIGURE 7. Effects of holding potential on outward current. (*A*) Time course of the slow inactivation process. The holding potential was −20 mV, the test potential was 40 mV, and the cell was stimulated every 5 s. At the arrow, the holding potential was set to −50 mV; the current recovered completely. (*B*) Amplitude of current at +40 mV following a 500-ms prepulse to different potentials. Records were taken 10 min after the whole-cell clamp was established. The cell was maintained at a holding potential of −80 mV. With a prepulse of 60 mV, corresponding to a starting potential of −20 mV, the amplitude of the outward current during the test pulse was ~50% of that from −80 mV. This value was subtracted from each current value to fit the points with the function: $I = I_{max}/\{1 + \exp[(V - V_{half})/K]\}$. The best fit gave $V_{half} = -44.4$ mV and $K = 5.6$ mV. The solutions were as in Fig. 2.

strong and Taylor, 1980). The effect of Ba^{2+} was reversible in all of the cells tested (three).

The outward current was also partially blocked by $CdCl_2$ (0.1–1 mM). Fig. 9*C* shows the inhibition of the outward current caused by different doses of $BaCl_2$ and $CdCl_2$ in representative cells held at −50 mV and depolarized to +10 mV for 50 ms. Cd^{2+} may block Ca^{2+}-dependent K^+ channels by inhibiting the Ca^{2+} influx through voltage-dependent Ca^{2+} channels. As described below, these cells do not seem to possess voltage-dependent Ca^{2+} channels, so $CdCl_2$ may act directly on the K^+ channel. Apamin (100 nM) also was tested, but it had no effect on the outward current or on the leak current.

Inward Currents

In a set of experiments aimed to characterize the inward components, Cs^+ was substituted for K^+ in the pipette. The internal solution contained 5 mM EGTA in these cases. In 90% of the cells, the only membrane current that persisted in these conditions was a voltage-independent, linear leak current, already mentioned. Only in 10% of the cells tested, the membrane current in voltage clamp exhibited a transient inward component, provided that the membrane potential was kept high enough (Fig. 10*A*). This inward current was blocked by 3 μM TTX (Fig. 10, *B–D*) and no TTX-resistant inward current was ever found, even

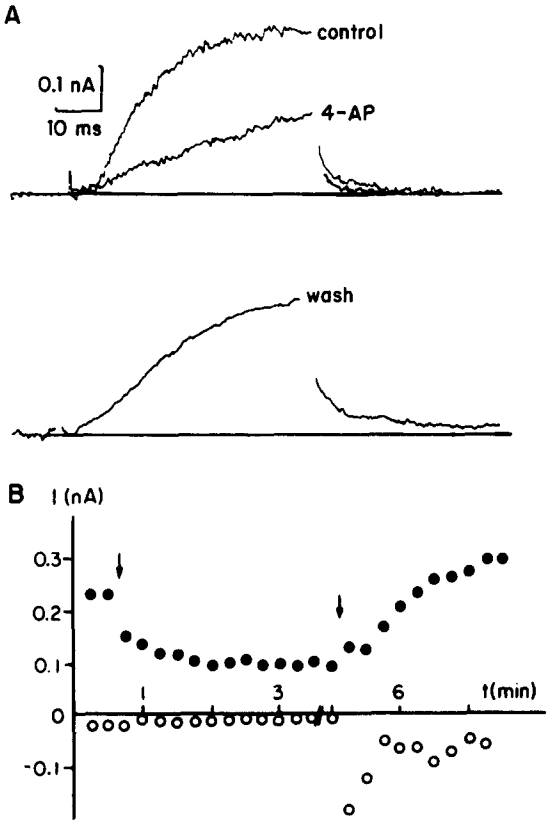

FIGURE 8. Inhibition of the outward current caused by 4-AP, in standard external (Tyrode) solution and standard internal (140 mM KCl, no EGTA) solution. (*A*) Current records before (control), during the application of 1 mM 4-AP, and after 5 min of wash. The holding potential was −50 mV and the test potential was 30 mV. (*B*) Time course of 4-AP inhibition of the outward current for the cell in *A*. Open circles: current at −50 mV; filled circles: current at 10 mV. The leak current at −50 mV increased during the wash and has been subtracted from the record shown in *A*.

at a high Ca^{2+} concentration (5 mM). This observation correlates with the finding that the outward current does not depend on external Ca^{2+}. The transient inward current displayed the features of a voltage-dependent Na^+ current, including fast activation and fast inactivation.

Single-Channel Recording

Single K^+ channel currents were recorded in both cell-attached and outside-out patches. In both cases, a single amplitude of current was detected at a given test potential. Fig. 11 shows single-channel currents from an outside-out patch that was held at −80 mV and depolarized to +20 mV for 300 ms. The holding

potential was chosen to maximize the probability of opening of the channels, which inactivated or ran down rapidly from more depolarized holding potentials. The bottom trace in Fig. 11 is the average of 30 idealized traces. The fit with n^2 kinetics gave a value of τ_n of 11.7 ms for this average trace. As is apparent from

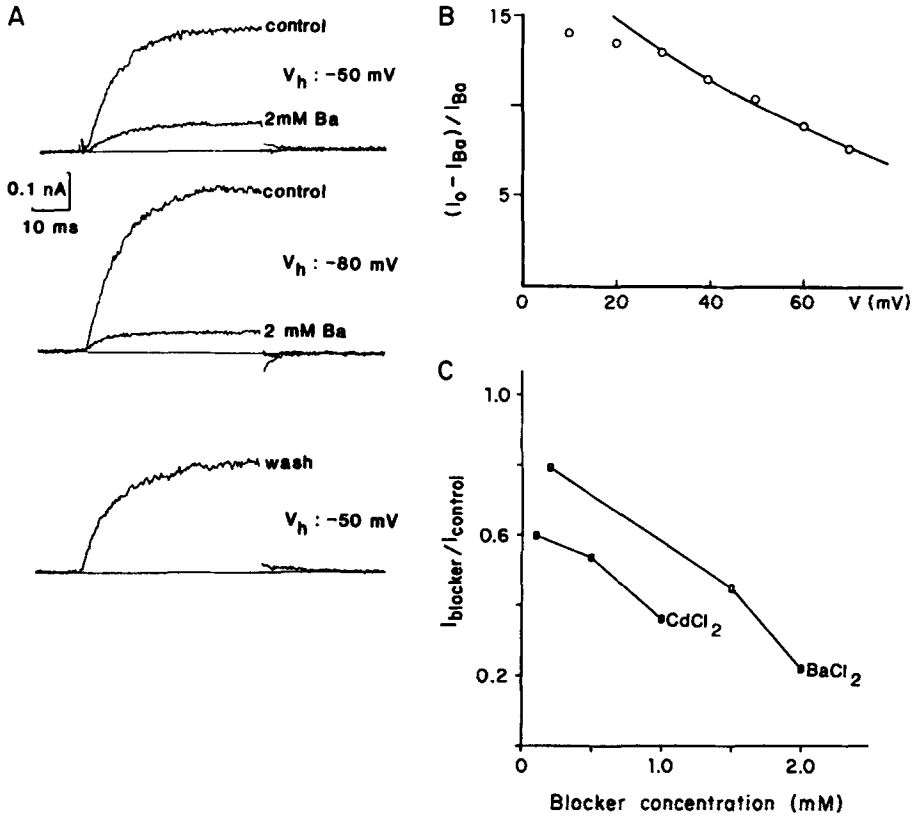

FIGURE 9. Inhibition of outward current produced by $BaCl_2$ and $CdCl_2$ in standard external and internal solutions. (*A*) Currents at 60 mV depolarization from holding potentials of −80 and −50 mV in control conditions, in the presence of 2 mM $BaCl_2$, and after wash (−50 mV only). (*B*) Voltage dependence of the Ba^{2+} block, from a holding potential of −80 mV. Points were fitted with an exponential curve according to the relation $(I_o - I_{Ba})/I_{Ba} = A\exp(-V/V')$, with $V' = 78$ mV. (*C*) Fractional inhibition of the outward current caused by different doses of Ba^{2+} and Cd^{2+}. For each blocker, the results from a representative cell that was exposed to increasing concentrations are shown. The cells were held at −50 mV. The values plotted are the amplitudes of the outward current at +10 mV in each condition. The current reached a steady state value ~20 s after the solution containing the divalent cation was introduced.

this figure, the average current reached maximum activation (steady state) ~100 ms after the onset of the pulse, and only events between 100 and 300 ms were used to calculate the kinetic parameters. The mean unitary current at +20 mV was 0.7 ± 0.1 pA in three patches (Fig. 12). Single channels in outside-out patches displayed bursting kinetics. The open-time distribution was fitted best

by a single-exponential decay, with a mean open time of 12 ± 1 ms at +20 mV (three patches). The distribution of closed times was biexponential, with τ_1 = 1.3 ± 0.2 ms and τ_2 = 15 ± 1 ms at +20 mV (three patches) (Fig. 12).

Fig. 13 shows how the single-channel conductance was calculated. Depolarizing steps to +20 mV were followed by a second step to +70 mV. The single-channel

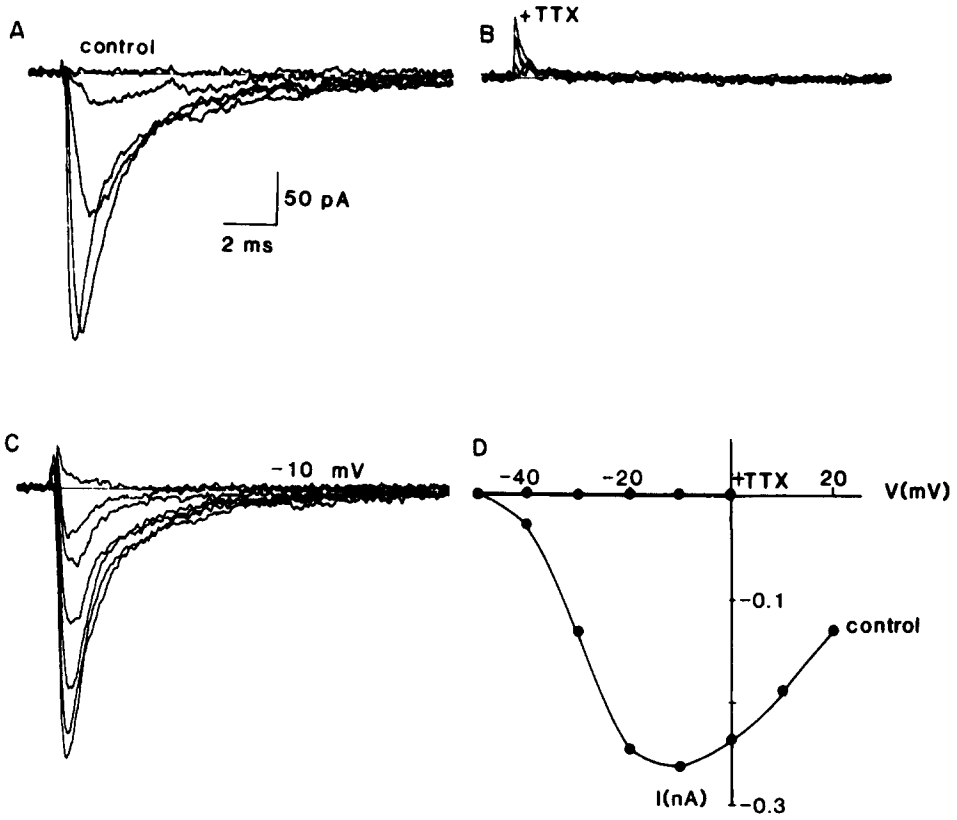

FIGURE 10. Inward membrane currents of an isolated hepatocyte. (*A*) Inward currents recorded from a cell held at −80 mV. External solution: standard Tyrode; pipette solution: CsAsp. Leak and capacitive currents have been subtracted. (*B*) Effect of the addition of 3 μM TTX to the bath. The test potential was −10 mV. Current traces were recorded every 15 s, 1–2 min after the perfusion with the solution that contained the drug was begun. (*C*) Current traces in the presence of TTX. (*D*) *I-V* relation for the inward current in *A* and *C*. In the presence of TTX, no inward component was detectable.

conductance calculated from the ratio $\Delta i/\Delta V$ was 7 pS in this patch. Similar experiments in three outside-out patches gave a mean unitary conductance of 7.0 ± 0.5 pS. When this value is compared with the estimated specific whole-cell conductance, a density of <1 (0.65) open channel/μm^2 results. Fig. 13*D* shows the voltage dependence of the unitary current in a cell-attached patch held at the resting membrane potential. The conductance estimated from the slope is 6.0 pS, which is close to the value obtained in outside-out patches.

DISCUSSION

In this work, we have demonstrated that dissociated hepatocytes from chick possess voltage-dependent outward currents carried mainly by K ions. No other ionic currents were present in the majority of the cells, apart from a leak conductance. This leak current could result from a decrease of the seal resistance as soon as the whole-cell clamp is established. However, we prefer to interpret it as an intrinsic conductance in the liver membrane, because it was always observed and was larger in cells with a larger area (estimated from the membrane capacitance). The observation that the liver cell membrane is intrinsically "leaky" may not be surprising, because of the high density of nonselective gap junction

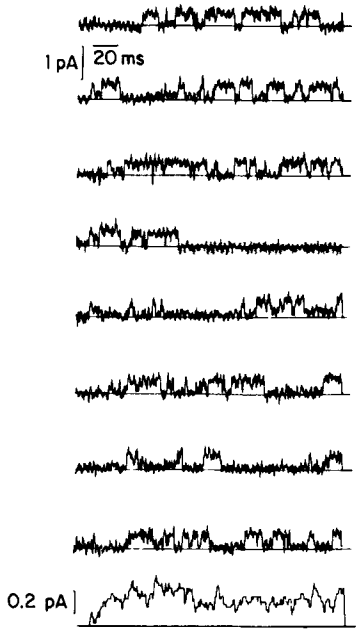

FIGURE 11. Single K^+ channel currents in an outside-out patch. The external bath was a standard solution, and the pipette contained 140 mM KCl, no EGTA. The patch was held at −80 mV. The single-channel currents were recorded at +20 mV. The bottom record is the mean of 30 idealized traces.

channels in these cells (Revel et al., 1980) and the possibility that not all of them sealed over during dispersion.

A voltage-dependent Na^+ current was also found in a small percentage of the cells. Its kinetics and TTX sensitivity suggest that it is not different from the Na^+ current found in excitable cells, but the description of this current is limited by its infrequent occurrence. This was the only inward current ever detected and we have found no evidence for voltage-dependent Ca^{2+} currents. Because the concentration of internal Ca^{2+} modulates many liver cell functions, a mechanism to supply Ca^{2+} from the external medium and replenish intracellular stores must be present. A mechanism different from a voltage-dependent channel has recently been postulated for rat liver (Hughes et al., 1986).

The K^+ current in chick hepatocytes closely resembles the delayed rectifier found in nerve and muscle cells, in its kinetics and sensitivity to blockers such as 4-AP and $BaCl_2$. A Hodgkin-Huxley–type model with n^2 kinetics was used to

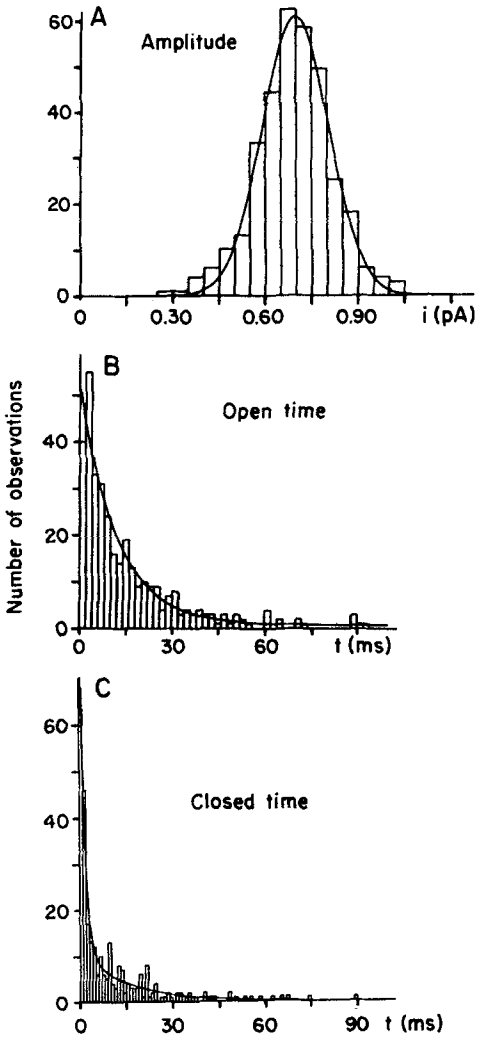

FIGURE 12. Histograms constructed from the idealized single K^+ channel currents shown in Fig. 11. Amplitude (*A*), open time (*B*), and closed time (*C*) histograms are shown. Histograms were fitted with a single Gaussian function, a single-exponential decay function, and a double-exponential decay function, respectively. The mean amplitude was 0.7 ± 0.1 pA, the mean open time was 12 ms, and the mean closed times were 1.5 and 16 ms.

FIGURE 13. Single K^+ channel conductance. (*A* and *B*) Single K^+ channel currents were recorded from an outside-out patch under the same conditions as Fig. 12. The patch was held at −80 mV, and depolarizing steps to +20 and +70 mV were applied successively. (*C*) The conductance, calculated from the ratio $\Delta i/\Delta V$, was 6.9 pS in this patch. (*D*) Mean unitary current as a function of voltage in a cell-attached patch. The single-channel current was estimated by eye for ~100 events at each potential and averaged. The linear regression has a slope of 6.0 pS.

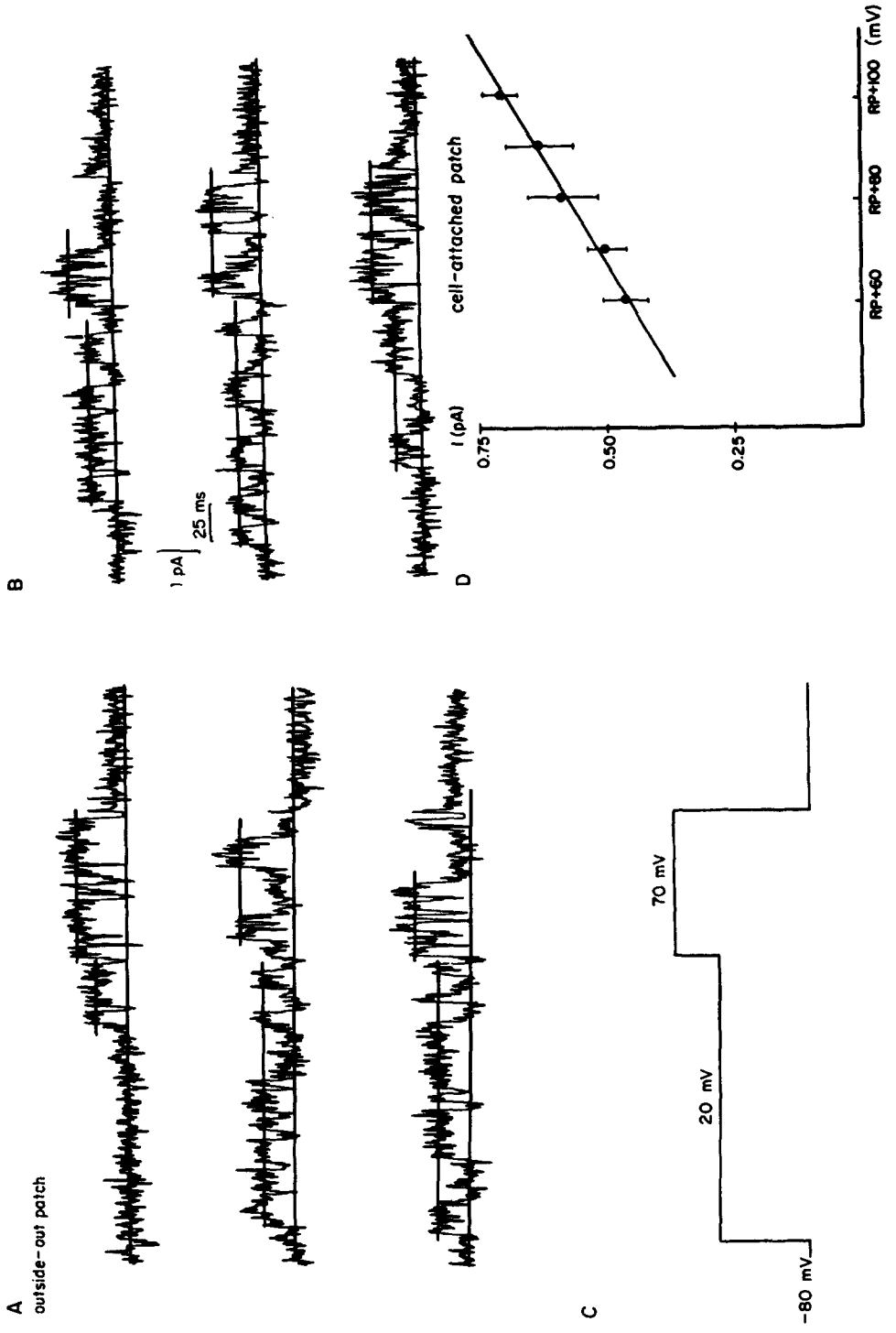
A
outside-out patch
B
1 pA
25 ms
C
70 mV
20 mV
-80 mV
D
cell-attached patch
I (pA)
0.75
0.50
0.25
RP+60
RP+80
RP+100 (mV)

describe the sigmoidal time course of the activation of this current, and a similar model had been used previously to describe the kinetics of the K^+ current in *Myxicola* axons (Schauf et al., 1976) and, more recently, the slowly rising K^+ current in single cardiac cells from frog atrium (Hume et al., 1986; Simmons et al., 1986). However, the hepatocyte K^+ current was fully activated in 200 ms, while the cardiac cell current required several seconds. The inactivation was negligible in 500 ms, but a reversible, slow inactivation was observed when the holding potential was maintained more positive than −40 mV for 1 min. Because this inactivation developed after some time, it may be a result of the recording conditions rather than an intrinsic property of the channel. In addition, part of the current was apparently inactivated at holding potentials more positive than −60 mV.

The K^+ current was independent of either the external or internal Ca^{2+} concentration. This conclusion is based on the assumption that the internal dialysis was adequate to buffer the Ca^{2+} in the entire cell interior. This condition was probably fulfilled, because in other experiments, using similar pipettes, the outward current was completely blocked by internal Cs^+. However, a local concentration of free Ca^{2+} higher than that of the bulk solution cannot be completely ruled out. Because of its Ca^{2+} independence and insensibility to apamin, the current described in this study does not resemble the K^+ current activated in response to Ca^{2+}-mobilizing hormones that has been identified in guinea pig hepatocytes (Burgess et al., 1981; DeWitt and Putney, 1984; Cook and Haylett, 1985). On the other hand, the response of the liver cells to the Ca^{2+}-mobilizing hormones varies from species to species, with significant differences between guinea pigs and rats (Burgess et al., 1981) and, to our knowledge, there are no reports concerning this response in avian hepatocytes.

Single channels of 7 pS conductance, with bursting kinetics, were found to be the unitary elements of this current. Voltage-dependent K^+ channels have been described in chromaffin cells (Marty and Neher, 1985), human lymphocytes (Cahalan et al., 1985), and macrophages (Ypey and Clapham, 1984). In chromaffin cells, at least three different K^+ channels have been identified, and the more conductive one was strongly Ca^{2+} dependent. This highly conductive channel is not found in lymphocytes and macrophages or in this hepatocyte preparation. Two pure voltage-dependent channels were found in both chromaffin cells and lymphocytes; the smaller one was the most similar to the K^+ channel recorded in these hepatocytes, in its conductance and slow inactivation.

We can speculate about the role of the voltage-dependent ionic conductances in liver function. Na^+ channels would be inactivated at a membrane potential close to the resting value and considerable hyperpolarizations would be required to remove the inactivation; also, their fast kinetics contrast with the relatively long-term liver function. In contrast, activation of the K^+ channels occurs near the resting membrane potential and does not require hyperpolarization. It can be triggered by any agent that causes a small depolarization of the membrane and could represent a negative feedback control on the membrane potential itself. We have made several attempts to correlate the K^+ conductance to hormone-driven functions. In particular, we have tested the actions of insulin (0.05–1 U/ml), glucagon (60–600 nM), and the α-adrenergic agonist phenyleph-

rine (0.5–10 μM), but none of these had any effect on the K^+ current in the whole-cell clamp condition. The action of these hormones is likely to involve more complex cellular mechanisms.

The authors thank Dr. R. Vick for help in revising the manuscript.

This work was supported by grants HL-36475 and NS-23877 to A. M. Brown.

Original version received 6 February 1987 and accepted version received 18 June 1987.

REFERENCES

Armstrong, C. M., and S. R. Taylor. 1980. Interaction of barium ions with K^+ channels in squid giant axons. *Biophysical Journal.* 30:473–488.

Berthon, B., T. Capiod, and M. Claret. 1985. Effects of noradrenaline, vasopressin and angiotensin on the Na-K^+ pump in rat isolated liver cells. *British Journal of Pharmacology.* 86:151–161.

Bevington, P. R. 1969. Data Reduction and Error Analysis for the Physical Sciences. McGraw-Hill, New York, NY. 204–246.

Brown, A. M., H. D. Lux, and D. L. Wilson. 1984. Activation and inactivation of single Ca^{2+} channels in snail neurons. *Journal of General Physiology.* 83:751–769.

Burgess, G. M., M. Claret, and D. H. Jenkinson. 1981. Effect of quinidine and apamin on the Ca-dependent K^+ permeability of mammalian hepatocytes and red cells. *Journal of Physiology.* 317:67–90.

Cahalan, M. D., K. G. Chandy, T. E. DeCoursey, and S. Gupta. 1985. A voltage-gated K^+ channel in human T lymphocytes. *Journal of Physiology.* 358:197–237.

Cook, N. S., and D. G. Haylett. 1984. Effect of apamin, quinin and neuromuscular blockers on Ca^{2+}-activated K^+ channels in guinea-pig hepatocytes. *Journal of Physiology.* 358:373–394.

DeWitt, L. M., and J. M. Putney. 1984. α-Adrenergic stimulation of K^+ efflux in guinea-pig hepatocytes may involve Ca^{2+} influx and Ca^{2+} release. *Journal of Physiology.* 346:395–407.

Edmondson, J. W., B. A. Miller, and L. Lumeng. 1985. Effect of glucagon on hepatic taurocholate uptake: relationship to membrane potential. *American Journal of Physiology.* 249:427–433.

Friedmann, N., and G. Dambach. 1980. Antagonist effect of insulin on glucagon evoked hyperpolarization. *Biochimica et Biophysica Acta.* 596:180–185.

Friedmann, N., A. V. Somlyo, and A. P. Somlyo. 1971. Cyclic adenosine and guanosine monophosphates and glucagon: effect on liver membrane potential. *Science.* 171:400–402.

Haber, R. S., and J. N. Loeb. 1986. Stimulation of K^+ efflux in rat liver by a low dose of thyroid hormone: evidence for enhanced cation permeability in the absence of Na, K-ATPase induction. *Endocrinology.* 118:207–211.

Hamill, O. P., A. Marty, E. Neher, B. Sakmann, and F. J. Sigworth. 1981. Improved patch-clamp technique for high resolution current recording from cell and cell-free membrane patches. *Pflügers Archiv.* 391:85–100.

Hughes, B. P., S. E. Milton, G. J. Barrit, and A. M. Auld. 1986. Studies with verapamil and nifedipine provide evidence for the presence in the liver cell plasma membrane of two types of Ca^{2+} inflow transporter which are dissimilar to potential operated Ca^{2+} channels. *Biochemical Pharmacology.* 35:3045–3052.

Hume, J. R., W. Giles, K. Robinson, E. F. Shibata, R. D. Nathan, K. Kanai, and R. Rasmusson. 1986. A time- and voltage-dependent K^+ current in single cardiac cells from bullfrog atrium. *Journal of General Physiology.* 88:777–798.

Krupp, M., and M. D. Lane. 1981. On the mechanism of ligand induced down regulation of insulin receptor level in the liver cell. *Journal of Biological Chemistry.* 256:1689–1694.

Lux, H. D., and A. M. Brown. 1984. Patch and whole cell calcium currents recorded simultaneously in snail neurons. *Journal of General Physiology.* 83:727–750.

Marty, A., and E. Neher. 1985. Potassium channels in bovine adrenal chromaffin cells. *Journal of Physiology.* 367:117–141.

Petersen, O. H. 1974. The effect of glucagon on the liver cell membrane potential. *Journal of Physiology.* 239:647–656.

Revel, J. S., S. B. Yanchey, D. J. Meyer, and M. Finbow. 1980. Behavior of gap junction during liver regeneration. *In* Communication of Liver Cells. H. Popper, L. Bianchi, F. Gudat, and W. Reutter, editors. MTP, Lancaster, England. 167–176.

Schauf, C. L., T. L. Pencek, and F. A. Davis. 1976. Potassium current kinetics in *Myxicola* axons. Effects of conditioning prepulses. *Journal of General Physiology.* 68:397–403.

Schlichter, L., N. Sidell, and S. Hagiwara. 1986. Potassium channels mediate killing by human natural killer cells. *Proceedings of the National Academy of Sciences.* 83:451–455.

Simmons, M. A., T. Creazzo, and H. C. Hartzell. 1986. A time-dependent and voltage-sensitive K^+ current in single cells from frog atrium. *Journal of General Physiology.* 88:739–755.

Somlyo, A. P., A. V. Somlyo, and N. Friedmann. 1971. Cyclic adenosine monophosphate, cyclic guanosine monophosphate, and glucagon: effects on membrane potential and ion fluxes in the liver. *Annals of the New York Academy of Sciences.* 185:1108–1145.

Tarlow, D. M., P. A. Watkins, R. E. Reed, R. S. Miller, E. E. Zwergel, and M. D. Lane. 1977. Lipogenesis and the synthesis and secretion of very low density lipoprotein by avian liver cells in nonproliferating monolayer culture. *Journal of Cell Biology.* 73:332–353.

Van Driessche, W., and W. Zeiske. 1985. Ionic channels in epithelial cell membranes. *Physiological Reviews.* 65:833–903.

Watkins, P. A., D. M. Tarlow, and M. D. Lane. 1977. Mechanism of acute control of fatty acid synthesis by glucagon and 3′:5′-cyclic AMP in the liver cell. *Proceedings of the National Academy of Sciences.* 74:1497–1501.

Williams, T. F., J. H. Exton, N. Friedmann, and C. R. Park. 1971. Effect of insulin and adenosine 3′,5′-monophosphate on K^+ flux and glucose output in perfused rat liver. *American Journal of Physiology.* 221:1645–1651.

Wondergem, R. 1983. Insulin depolarization of rat hepatocytes in primary monolayer culture. *American Journal of Physiology.* 244:C17–C23.

Wondergem, R., and D. R. Harper. 1980. Transmembrane potential and amino acid transport in rat hepatocytes in primary culture. *Journal of Cellular Physiology.* 104:53–60.

Yeh, J. Z., G. S. Oxford, C. H. Wu, and T. Narahashi. 1976. Dynamics of aminopyridine block of K^+ channels in squid axon membrane. *Journal of General Physiology.* 68:519–535.

Ypey, D. L., and D. E. Clapham. 1984. Development of a delayed outward-rectifying K^+ conductance in cultured mouse peritoneal macrophages. *Proceedings of the National Academy of Sciences.* 81:3083–3087.